Supporting information

Flow stabilizer on a syringe tip for hand-powered microfluidic sample injection

Nan Xiang, Yu Han, Yuan Jia, Zhiguo Shi, Hong Yi, and Zhonghua Ni

School of Mechanical Engineering, and Jiangsu Key Laboratory for Design and Manufacture of Micro-Nano Biomedical Instruments, Southeast University, Nanjing, 211189, China.

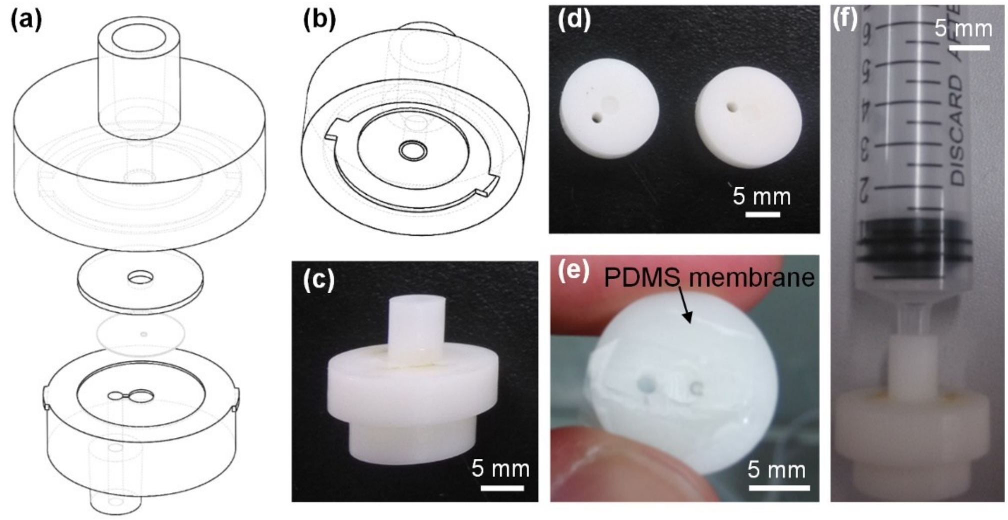

Figure S1. (a) CAD drawing of our syringe flow-stabilizer for clearly illustrating the detailed structure design. (b) CAD drawing of the inlet housing. (c) Photograph of the finally assembled prototype of our syringe flow-stabilizer in which the two housings were fabricated in photocurable resins using the 3D printing technique. (d) Photographs of the 3D-printed outlet housings with differently-sized deformation cavities. (e) Photograph of the outlet housing with a layer of PDMS membrane covering on its upper surface. (f) Photograph of our syringe flow-stabilizer connected with a 10 ml plastic syringe for hand-powered sample injection.

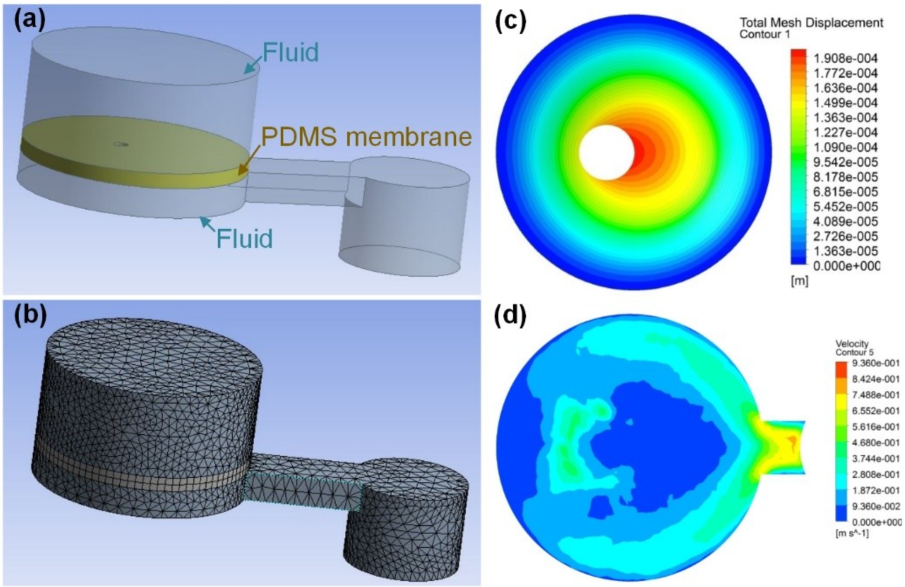

Figure S2. (a) Nonlinear model of Fluid–Structure Interaction (FSI) for simulating the membrane deformation and the fluid velocity in the deformation cavity. (b) Result of finite-element method (FEM) mesh generation. (c) Numerical simulation result of the membrane deformation (vertical view). (d) Numerical simulation result of the flow velocity in the deformation cavity (vertical view).

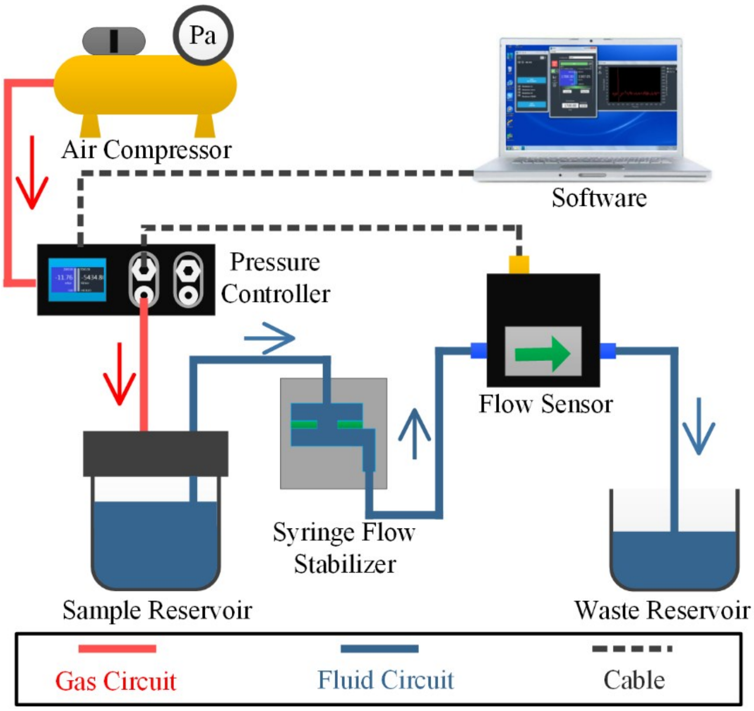

Figure S3. The gas-driven flow system for characterizing the performance of our syringe flow-stabilizer. The compressed air was regulated via a computer-controlled pressure controller to generate a specific pressure for driving the sample in the sealed sample reservoir. The sample was then flow through our syringe flow-stabilizer and the output flow rate was measured using a flow sensor. The values of pressures and flow rates were monitored and recorded using the software. The pressures generated by handedly pushing the syringe were measured via injecting the gas into the pressure controller (the function of feedback control is closed so that the pressure controller only measures and displays the pressure values). The pressure values generated from over five operators with different ages and body mass indexes were measured.

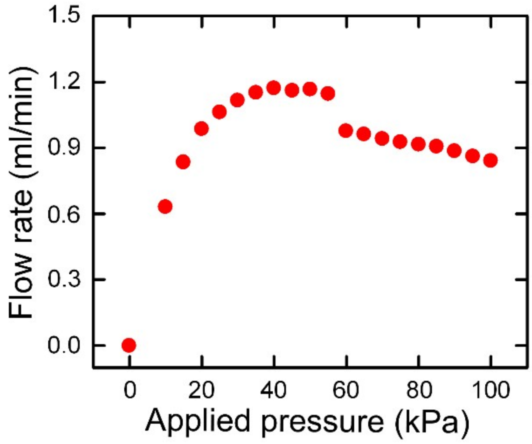

Figure S4. Output flow rates of our previously reported five-layer flow regulator ((100-300)100, i.e., the height of the main channel is 100 μm, the contraction gap width is 100 μm and the membrane length is 300 μm) at different applied pressures ranging from 0~100 kPa. When the applied pressure was increased to be larger than 100 kPa, the regulator broke down.

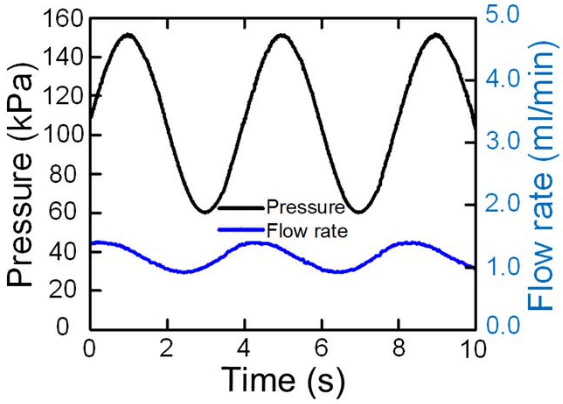

Figure S5. Output flow rate of the device H100D200 under the sinusoidal wave pressures with an extremely large amplitude of 90 kPa (changing from 60 kPa to 150 kPa) and the frequency of 0.25 s^{-1}.

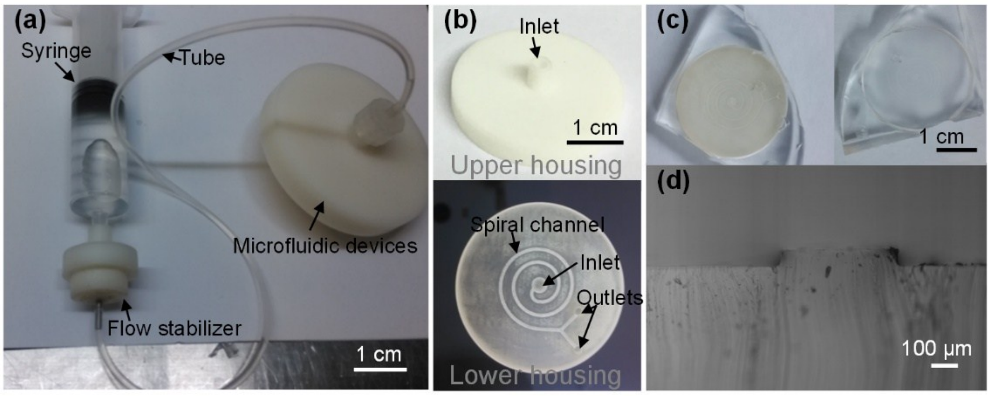

Figure S6. (a) Method for connecting the syringe flow-stabilizer with other microfluidic devices (e.g., inertial microfluidic cell concentrator or the most popular PDMS microfluidic devices) via tubings and fittings. (b) Photographs of the upper and lower housings fabricated via 3D printing. The inlet locates at the center of the upper housing. The semi-open spiral channel with one inlet and two outlets are on the upper surface of the lower housing. (c) Method for replicating the microchannel on the lower housing. The degassed PDMS mixture was poured onto the upper surface of the lower housing. After curing, the PDMS block was peeled from the lower housing and cut to observe the cross-sectional profile. (d) Microscopic image illustrating the cross-sectional profile of the spiral channel in 3D printed lower housing.

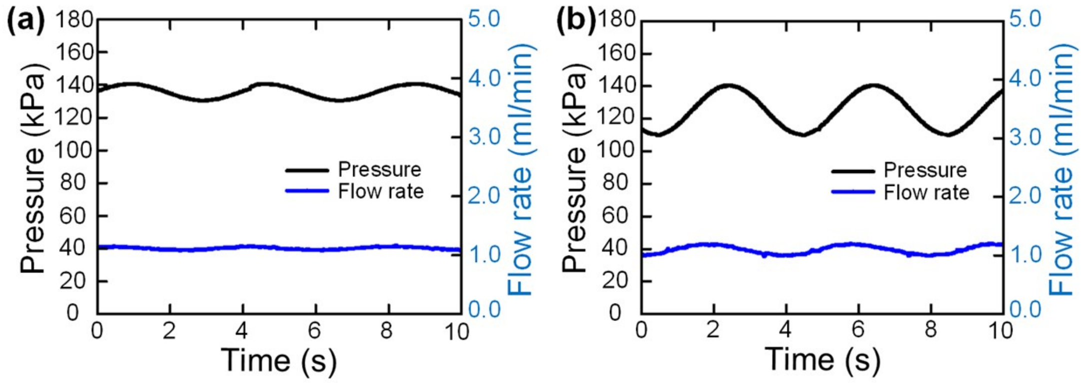

Figure S7. Output flow rates of the integrated device under the sinusoidal wave pressures with amplitudes changing from (a) 130 kPa to 140 kPa and (b) 110 kPa to 140 kPa. The frequency of the two sinusoidal wave pressures is fixed to be 0.25 s^{-1}.

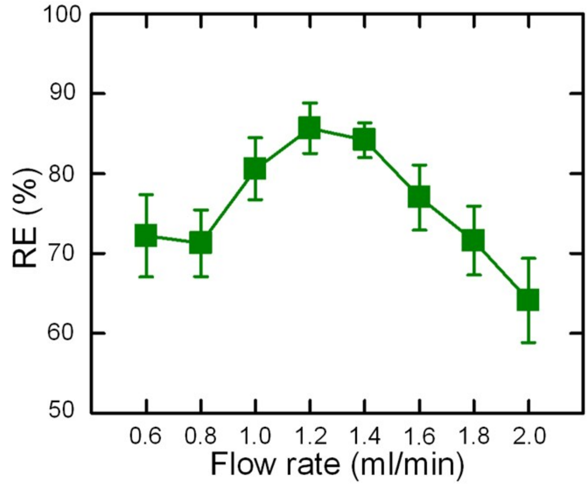

Figure S8. Cell recovery efficiency (RE) of our 3D printed inertial microfluidic cell concentrator under different flow rates for determining the optimal operating flow rate. The driving flow rate in this experiment was provided by the syringe pump and was controlled to be in the range of 0.6~2.0 ml/min.